中国激光

全保偏掺铒光纤皮秒脉冲及高效率倍频技术研究

杨占军[1]，郝强[1*]，汤成[1]，俞冰昊[1]，曾和平[1,2,3]

[1]上海理工大学光电信息与计算机工程学院，上海 200093；

[2]华东师范大学精密光谱科学与技术国家重点实验室，上海 200062；

[3]济南量子技术研究院，山东 济南 250101

摘要 实验搭建了基于全保偏掺铒光纤激光器的高效率倍频光源。采用可饱和吸收镜进行锁模，并通过两级掺铒光纤放大器实现了高重复频率、窄光谱的线偏振皮秒脉冲输出。在 PPLN 晶体中对该脉冲进行倍频处理，获得了光谱宽度为 0.68 nm、中心波长为 774.8 nm 的皮秒脉冲，平均功率为 613 mW，最大转换效率为 55.7%，倍频脉冲在 3 h 内平均功率的相对抖动低至 0.6%。该光源具有结构紧凑、稳定性高的优势，可应用于超快光谱学、半导体测试等领域。

关键词 激光器；光纤激光器；倍频；全保偏；皮秒脉冲

中图分类号 O437 **文献标识码** A **doi**：10.3788/CJL202148.1315003

脉冲宽度在皮秒量级的 780 nm 波段激光在太赫兹时域光谱[1]、材料微加工[2]和相干反斯托克斯拉曼散射（CARS）成像[3-4]等多个领域中有着重要的应用。钛宝石激光器可直接产生 780 nm 波段皮秒脉冲[5]，但其光路为空间结构，对环境敏感，需要配置隔振平台及恒温实验室。与钛宝石激光器相比，光纤激光器具有结构紧凑、光束质量好、抗干扰能力强等优点。特别是掺铒光纤激光器的发射波长为 1.5 ～1.6 μm，通过光学倍频可产生 780 nm 波段[6-8]脉冲。基于准相位匹配技术[9-10]的周期性极化晶体可有效规避基频光和倍频光的波矢失配，实现高效率的倍频激光（SHG）输出，因此受到研究人员的青睐。Zhang 等[11]采用腔内主动锁模，产生了脉宽为 60 ps、重复频率为 6.12 GHz 的 1550 nm 脉冲；并通过 10 mm 长度的 PPLN 晶体，倍频输出了 150 mW 的 775 nm 皮秒脉冲，转换效率为 23.4%。Hu 等[12]采用马赫-曾德尔调制器对 1560 nm 连续光进行调制，获得了脉宽为 430 ps、重复频率为 50 MHz 的脉冲光；并通过 35 mm 长度的 PPLN 晶体，倍频获得了 3.5 W 的 780 nm 脉冲。由于该系统采用非保偏光纤结构，转换效率仅为 22.4%，且易受环境干扰，功率稳定性欠佳。Hansknecht 等[13]通过增益开关调制分布式反馈（DFB）激光器，产生了脉宽为 40 ps、重复频率为 499 MHz 的 1560 nm 脉冲；该系统基于全保偏光纤结构，利用 10 mm 长的 PPLN 晶体，倍频获得了 2 W 的 780 nm 脉冲，转换效率为 40%。Lecourt 等[14]采用可饱和吸收镜进行锁模，并以 Sagnac 环作为端镜，经光学滤波后获得了脉宽为 15.5 ps、重复频率为 55 MHz 的 1560 nm 皮秒脉冲；通过 MgO-PPLN 晶体输出了 700 mW 的倍频光，转换效率为 35%。本文搭建了基于全保偏掺铒光纤激光器的倍频装置，采用可饱和吸收镜进行锁模，并以光纤布拉格光栅作为滤波反射镜，经两级光纤放大后，获得了高重复频率、窄光谱的近红外皮秒脉冲。该脉冲在 PPLN 晶体中，通过倍频产生了最大功率为 613 mW 的 775 nm 脉冲，转换效率高达 55.7%。

实验装置如图 1 所示，包括掺铒光纤激光器和光学倍频两部分结构。掺铒光纤激光器如图 1(a) 所示，SESAM 为可饱和吸收镜，中心波长为 1550 nm，带宽为 20 nm；WDM 为波分复用器；ESF 为长度为 0.9 m 的单模保偏掺铒光纤；光纤

收稿日期：2021-03-15；**修回日期**：2021-04-11；**录用日期**：2021-04-19

基金项目：国家重点研发计划（2018YFB0407100）、国家自然科学基金（11727812）

通信作者：*qianghao@usst.edu.cn

布拉格光栅（FBG）的中心波长和带宽分别为1550 nm和1 nm。LD为中心波长为974 nm的激光二极管，最大输出功率为400 mW。实验使用的保偏光纤为波长为1550 nm的单模光纤，纤芯直径为8.5 μm。振荡器为线性腔结构，通过SESAM锁模[15]实现了种子脉冲输出。种子脉冲经单模掺铒光纤放大器（EDFA）提升功率后注入主放大器中，为后续倍频提供基频光。为了防止后向传输光影响锁模状态，在振荡器和放大器之间插入光纤隔离器（ISO）。主放大器的泵浦源为高功率激光二极管（HP-LD），最大输出功率为9 W。倍频装置如图1（b）所示，基频光经L1透镜准直后，利用半波片（HWP）将其调节为竖直偏振状态以满足准相位匹配条件；L2透镜的焦距为19 mm，将基频光聚焦至周期极化铌酸锂（PPLN）晶体内；PPLN的反转周期为19.34 μm，尺寸为10 mm×3 mm×1 mm。为了避免环境温度的干扰，晶体放置于控温精度为0.1 ℃的温控炉（Oven）中。倍频光和剩余基频光经透镜L3准直后被两面二向色镜（DM1、DM2）分束。

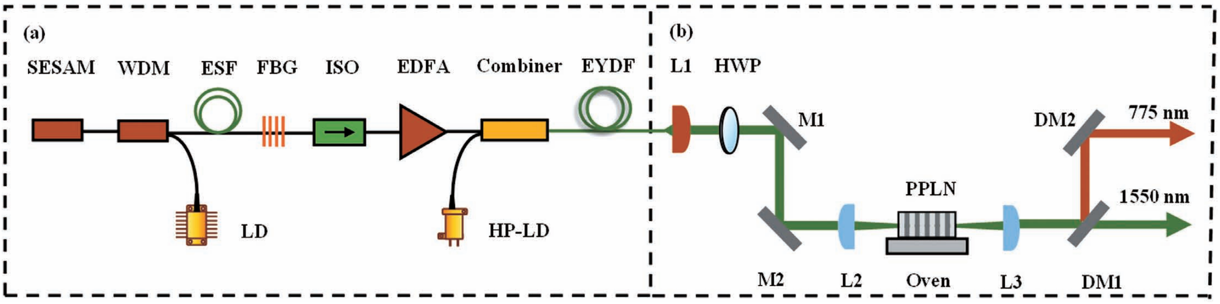

图1　实验装置。（a）掺铒光纤激光器；（b）倍频装置

Fig. 1　Experimental setup. (a) Er-doped fiber laser; (b) SHG device

在实验中，当激光二极管（LD）的功率达到298 mW后，振荡器实现锁模自启动，产生的激光脉冲的重复频率为100 MHz、平均功率为30 mW。输出脉冲经EDFA后，平均功率被提升至百毫瓦量级。主放大器采用长度为2 m的双包层铒镱共掺（EYDF）光纤作为增益介质，有效提高了光-光转换效率并抑制了光纤中的非线性效应。当HP-LD的功率为7 W时，输出脉冲的平均功率为1.3 W。如图2（a）、（b）所示，基频光的中心波长为1549.6 nm，光谱宽度为1.01 nm，相应的脉冲宽度为11.6 ps(假定为高斯脉冲)。由于脉冲的产生和放大均采用保偏光纤，基频光的偏振对比度可达13 dB。为了降低高功率泵浦导致的晶体损伤风险，后续倍频时基频光的最大入射功率为1.1 W。

基频光通过PPLN晶体实现频率转换，产生的倍频光的中心波长为774.8 nm、光谱宽度为0.68 nm，相应的脉冲宽度为11.4 ps，如图2（c）、（d）所示。

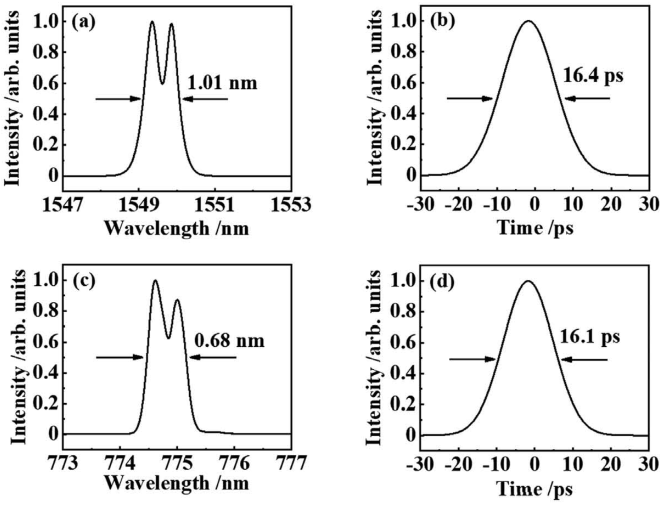

图2　光谱和脉宽。（a）基频光光谱；（b）基频光脉宽；（c）倍频光光谱；（d）倍频光脉宽

Fig. 2　Spectrum and pulse duration. (a) Spectrum of fundamental wave; (b) pulse duration of fundamental wave; (c) spectrum of SHG; (d) pulse duration of SHG

在倍频光路中，通过微调光路确定出基频光斑在 PPLN 晶体内的最佳位置，而短焦距的聚焦透镜有效提高了入射脉冲的峰值功率密度。PPLN 晶体的长度为 10 mm，既保证基频光与晶体有足够长的作用距离，又避免了基频光光谱的损失。之后通过温控炉调节晶体温度，获得了高转换效率的倍频光。此外，基频光的高偏振对比度也对转换效率的提高起到了关键性的作用。图 3(a)展示了倍频光的输出功率和转换效率随基频光功率的变化。实验发现，倍频光的功率随基频光功率的增加而单调增加。当基频光功率大于 700 mW 时，转换效率表现出一定的饱和效应。当基频光功率为 1.1 W 时，转换效率达到最高，为 55.7%，此时倍频光的输出功率为 613 mW。由于非线性频率转换对偏振极为敏感，倍频光的偏振对比度达 27 dB。此外，实验测量了倍频光的功率与晶体温度的关系，如图 3(b)所示，当晶体温度达到 34 ℃时，倍频光的转换效率最高。当倍频光的输出功率为 613 mW 时，通过光斑分析仪在准直透镜 L3 后 1 m 处测量了倍频光的光斑，如图 3(b)中插图所示，倍频光的光斑直径为 0.92 mm，圆度为 97%。得益于稳定的锁模机制和全保偏的光纤结构，倍频脉冲表现出良好的功率稳定性。如图 3(c)所示，倍频脉冲在 3 h 测量时间内平均功率的相对抖动 σ 低至 0.6%，短时间内的峰峰值波动为 2 mW。为了进一步拓展应用，将系统集成于尺寸为 330 mm×250 mm×110 mm 的机箱中，实现了小型化封装，如图 3(d)所示。

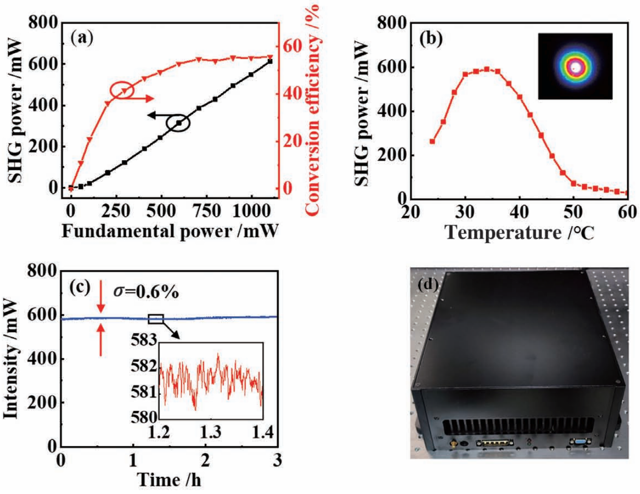

图 3　实验结果。(a)倍频光功率和相应的转换效率随基频光功率的变化；(b)倍频光功率与晶体温度的关系及光斑(插图)；(c)倍频光功率稳定性；(d)实物图

Fig. 3　Experimental results. (a) SHG power and corresponding conversion efficiency versus fundamental-wave power; (b) SHG power versus crystal temperature and facula (inset); (c) SHG power stability; (d) photo of product

综上所述，实验验证了基于全保偏掺铒光纤激光器的高效率倍频方案，利用 PPLN 晶体获得了中心波长为 774.8 nm 的皮秒脉冲，转换效率高达 55.7%。所提方案基于全保偏光纤结构，具有紧凑性、便捷性、稳定性等优点，可替代部分钛宝石激光器。

参　考　文　献

[1] Tadokoro Y, Takida Y, Kumagai H, et al. Comparative study on THz time-domain spectroscopy using 780-nm 1.3-ps laser pulses with different detections of LT-GaAs photoconductive antenna and ZnTe electro-optic sampling [J]. Proceedings of SPIE, 2013, 8604: 86040D.

[2] Shaheen M E, Gagnon J E, Fryer B J. Laser ablation of iron: a comparison between femtosecond and picosecond laser pulses [J]. Journal of Applied Physics, 2013, 114(8): 083110.

[3] Krauss G, Hanke T, Sell A, et al. Compact coherent anti-Stokes Raman scattering microscope based on a picosecond two-color Er : fiber laser system [J]. Optics Letters, 2009, 34(18): 2847-2849.

[4] Zheng S K, Yang K W, Ao J P, et al. Advances in fiber laser sources for coherent Raman scattering microscopy[J]. Chinese Journal of Lasers, 2019, 46(5): 0508008.
郑世凯, 杨康文, 敖建鹏, 等. 光纤式相干拉曼散射成像光源研究进展[J]. 中国激光, 2019, 46(5): 0508008.

[5] Liu H G, Hu M L, Song Y J, et al. Operation of Kerr-lens mode-locked Ti: sapphire laser in the non-

soliton regime[J]. Chinese Physics B, 2010, 19(1): 014215.

[6] Champert P A, Popov S V, Taylor J R. Highly efficient, variable pulse format, 770-nm source based on powerful seeded fiber amplifier and second-harmonic generation in periodically poled KTP[C]//Conference on Lasers and Electro-Optics (CLEO 2000), May 7-12, 2000, San Francisco, CA, USA. New York: IEEE Press, 2000: 424-425.

[7] Fang Q, Cui X L, Zhang Z, et al. 97-μJ single frequency linearly polarized nanosecond pulsed laser at 775 nm using frequency doubling of a high-energy fiber laser system[J]. Optical Engineering, 2017, 56(8): 086112.

[8] Wu J R, Lü Z Q, Lu X, et al. Characteristics of second harmonic generation in erbium doped femtosecond fiber lasers based on quasi phase matching[J]. Chinese Journal of Lasers, 2018, 45(7): 0701001.
吴嘉瑞, 吕志强, 陆星, 等. 基于准相位匹配的掺铒飞秒光纤激光器倍频特性研究[J]. 中国激光, 2018, 45(7): 0701001.

[9] Zhu S N, Zhu Y Y, Ming N B. Quasi-phase-matched third-harmonic generation in a quasi-periodic optical superlattice[J]. Science, 1997, 278(5339): 843-846.

[10] Guo S L, Han Y S, Wang J, et al. Investigation of quasi-phase-matching frequency doubling of 1560 nm laser by use of PPLN and PPKTP crystals[J]. Acta Optica Sinica, 2012, 32(3): 0319001.
郭善龙, 韩亚帅, 王杰, 等. 1560 nm 激光经 PPLN 和 PPKTP 晶体准相位匹配倍频研究[J]. 光学学报, 2012, 32(3): 0319001.

[11] Zhang S G, Yao J H, Liu Y G, et al. Fiber-format pico-second source based on efficient frequency doubling of a high-repetition rate erbium-fiber laser amplifier[J]. Microwave and Optical Technology Letters, 2011, 53(1): 169-171.

[12] Hu D J J, Murray R T, Legg T, et al. Fiber-integrated 780 nm source for visible parametric generation[J]. Optics Express, 2014, 22(24): 29726-29732.

[13] Hansknecht J, Poelker M. Synchronous photoinjection using a frequency-doubled gain-switched fiber-coupled seed laser and ErYb-doped fiber amplifier[J]. Physical Review Special Topics- Accelerators and Beams, 2006, 9(6): 063501.

[14] Lecourt J B, Dortu F, Ouinten C E, et al. Switchable dual wavelength picosecond fiber laser source operating around 780 nm for advanced Raman spectroscopy[J]. Proceedings of SPIE, 2019, 10908: 109080M.

[15] Luo J, Yang S, Hao Q, et al. Precise locking the repetition rate of a SESAM mode-locking all polarization maintaining fiber laser[J]. Acta Optica Sinica, 2017, 37(2): 0206003.
罗浆, 杨松, 郝强, 等. SESAM 锁模全保偏光纤激光器重复频率的精确锁定[J]. 光学学报, 2017, 37(2): 0206003.

Picosecond Pulse and High Efficiency Frequency Doubling Based on All-Polarization-Maintaining Er-Doped Fibers

Yang Zhanjun[1], Hao Qiang[1*], Tang Cheng[1], Yu Binghao[1], Zeng Heping[1,2,3]

[1] *School of Optical Electrical and Computer Engineering, University of Shanghai for Science and Technology, Shanghai* 200093, *China*;

[2] *State Key Laboratory of Precision Spectroscopy Science and Technology, East China Normal University, Shanghai* 200062, *China*;

[3] *Jinan Institute of Quantum Technology, Jinan, Shandong* 250101, *China*

Abstract

Objective A picosecond pulse at 780 nm has played an important role in practical applications and scientific researches. A Ti: sapphire laser is a famous light source at this wavelength range. However, due to its bulk design and complex architecture, the Ti: sapphire laser is sensitive to its environment. Compared with Ti: sapphire lasers, fiber lasers have the advantages of compact structure, high beam quality, and high stability. An alternative way to generate a picosecond pulse at 780 nm is to utilize frequency doubling of the pulse output from an Er-doped fiber laser. In this study, we experimentally demonstrated a frequency doubling efficiency as high as 55.7% based on an all-polarization-maintaining Er-doped fiber laser. Moreover, this scheme favors the advantages such as compact structure and good stability, and can be further applied in many fields such as ultrafast spectroscopy and semiconductor testing.

Methods In this study, a passively mode-locked fiber oscillator and a cascaded fiber amplifier, including a single mode fiber pre-amplifier and a double-cladding fiber amplifier, were used to produce a picosecond pulse at 1550 nm. The fiber oscillator was mode-locked by a semiconductor saturable absorber mirror (SESAM). A segment of Er-Yb co-doped double-cladding fiber with a 12 μm fiber core was used in the main amplifier to provide a laser gain and suppress nonlinear effects at a watt-level average power. The frequency conversion was achieved in a periodically poled lithium niobate (PPLN) crystal with 10 mm × 3 mm × 1 mm size and a 19.34 μm poling period. The fundamental-wave was focused on the PPLN crystal by a lens with a 19 mm focal length. A temperature-controlled oven was used to achieve the thermal phase matching condition for frequency doubling. A collimating lens and two dichroic mirrors were used for splitting the two beams at 775 nm and 1550 nm.

Results and Discussions The average power from the oscillator was 30 mW at a 100-MHz repetition rate. Subsequently, the pulsed laser was amplified to 1.3 W by the cascaded Er-doped fiber amplifiers. The amplified pulse had a spectral bandwidth of 1.01 nm centered at 1549.6 nm, and a pulse duration of 11.6 ps [Fig. 2(a) and Fig. 2(b)]. The polarization extinction ratio of the pulse was measured to be 13 dB. In order to avoid optical damage on the end facet of the crystal, the maximum incident power of the fundamental-wave was controlled below 1.1-W average power. The optimum temperature of this PPLN crystal was 34 ℃. In our experiment, the second harmonic average power increases monotonically with the fundamental-wave power. With an incident average power of 1.1 W, the second harmonic laser achieves a power as high as 613 mW, yielding a conversion efficiency of 55.7% [Fig. 3(a)]. The spectral bandwidth and pulse duration of the frequency doubled pulse are 0.68 nm and 11.4 ps, respectively [Fig. 2(c) and Fig. 2(d)]. Benefiting from the all-polarization-maintaining fiber architecture, the frequency doubled pulse exhibits an excellent long-term stability. As shown in Fig. 3(c), the average power instability is as low as 0.6% within 3 h.

Conclusions A picosecond laser architecture for 780-nm spectral range was demonstrated by using an all-polarization-maintaining Er-doped fiber laser and a PPLN frequency doubling crystal. As high as 613-mW average power and 55.7% conversion efficiency were achieved. The proposed laser scheme has the characteristics of compact structure and high stability, which is a good candidate to replace Ti:sapphire lasers in some circumstances.

Key words lasers; fiber lasers; second harmonic generation; all polarization-maintaining; picosecond pulse

OCIS codes 140.3510; 140.3515; 320.7090; 060.2420